

LIFETIME MEASUREMENTS IN  $^{42}\text{Sc}$ N. R. ROBERSON<sup>†</sup> and G. VAN MIDDELKOOP*Fysisch Laboratorium, Rijksuniversiteit, Utrecht, The Netherlands*

Received 2 September 1971

**Abstract:** Levels of  $^{42}\text{Sc}$  were populated with the  $^{40}\text{Ca}(\tau, p)^{42}\text{Sc}$  reaction at  $E_\tau = 8.4$  and 8.6 MeV. Gamma rays were measured in coincidence with protons. From Doppler-shift attenuation measurements mean lifetimes (or limits) have been obtained for 15 levels below  $E_x = 4$  MeV. Also, for many states accurate (1–2 keV) excitation energies were obtained. The lifetimes have been compared with calculations based on the wave functions of Flowers and Skouras which have both spherical and deformed components.

E NUCLEAR REACTION  $^{40}\text{Ca}(\tau, p\gamma)$ ,  $E = 8.4$  and 8.6 MeV; measured  $E_\gamma(\theta)$ , Doppler-shift attenuation,  $^{42}\text{Sc}$  deduced levels,  $T_{1/2}$ . Natural target.

## 1. Introduction

Recent calculations by Flowers and Skouras <sup>1)</sup> for  $^{42}\text{Ca}$  and  $^{42}\text{Sc}$ , have described a number of states in these nuclei as mixtures of 4p-2h deformed and 2p spherical shell-model components. The results of these calculations are in rather good agreement with the measured positive-parity spectrum and the electromagnetic transition rates in  $^{42}\text{Ca}$ . The model also explains many of the large number of low-lying levels of  $^{42}\text{Sc}$  [refs. <sup>2–7)</sup>]. However, the lack of experimental information prevented a detailed comparison.

In a continuation of an earlier study <sup>5)</sup>, Sherr *et al.* <sup>8)</sup> have carried out a high-resolution (9 keV) investigation of the  $^{42}\text{Ca}(\tau, t)^{42}\text{Sc}$  reaction at  $E_\tau = 26$  MeV. Combining these results with those of various other investigations <sup>6, 7, 9)</sup> Sherr *et al.* deduced a level scheme of  $^{42}\text{Sc}$  with at least 45 levels below 4.0 MeV (not counting doublets). Using the wave functions of Flowers and Skouras <sup>1)</sup> and Pühlhofer <sup>6)</sup>, a microscopic analysis of the  $(\tau, t)$  reaction data has subsequently been carried out by Schaeffer <sup>10)</sup>.

The early information available about  $\gamma$ -ray transitions has been summarized by Endt and Van der Leun <sup>11)</sup>. Two recent  $\gamma$ -ray angular-correlation studies using the  $^{40}\text{Ca}(\tau, p)^{42}\text{Sc}$  reaction have been carried out by Nicholas *et al.* <sup>9)</sup> and Balamuth *et al.* <sup>12)</sup> for levels below 2.3 MeV. Lifetime measurements for the levels at 0.61, 1.49, 1.51, 1.59 and 1.89 MeV have been reported by Grawe *et al.* <sup>13)</sup>.

The present paper describes a study of some of the levels of  $^{42}\text{Sc}$  below 4.0 MeV with the  $^{40}\text{Ca}(\tau, p\gamma)^{42}\text{Sc}$  reaction ( $Q = 4.90$  MeV). The primary purpose of the present investigation was the measurement, with the Doppler-shift attenuation

<sup>†</sup> On leave from Duke University and the Triangle Universities Nuclear Laboratory, Durham, N.C.

(DSA) method, of the lifetimes of these levels. For many states these measurements also yield accurate (1–2 keV) excitation energies. While the geometry of the experimental apparatus did not allow branching-ratio measurements, main decay modes were either reconfirmed<sup>2, 5, 9, 12)</sup> or determined for the levels studied. A comparison has been made with the lifetimes as computed for  $^{42}\text{Sc}$  by Flowers and Skouras<sup>1)</sup>.

## 2. The experimental procedure

The general experimental procedure has been described previously<sup>14)</sup> and only the salient features will be discussed here.

Calcium targets were prepared in vacuum by evaporating natural calcium metal from a Ta boat onto  $140\text{ }\mu\text{g}/\text{cm}^2$  carbon foils. When the evaporation was completed, the evaporating system was filled with argon and the target sealed in a small glass bottle. The glass bottle was placed in the scattering chamber, and the chamber was flushed with argon gas for approximately 1 h. After the removal of the glass bottle, the chamber was evacuated. Targets were prepared by this method immediately before bombardment and showed no appreciable oxidation after 4 d. Two different targets were used: (i)  $170\text{ }\mu\text{g}/\text{cm}^2$  of Ca for the measurements at  $E_{\tau} = 8.6\text{ MeV}$  and (ii)  $150\text{ }\mu\text{g}/\text{cm}^2$  at  $E_{\tau} = 8.4\text{ MeV}$ . The target thickness was determined from the frequency shift of a Sloan crystal thickness gauge placed at the same distance from the Ta boat as the target. The thickness of the carbon foils was obtained from the measured energy loss of  $5.48\text{ MeV}$   $\alpha$ -particles.

A beam of  $^3\text{He}^{++}$  particles from the Utrecht 6 MV tandem Van de Graaff accelerator was used at bombarding energies between 7.0 and 10.0 MeV to study the reaction  $^{40}\text{Ca}(\tau, p\gamma)^{42}\text{Sc}$ . The beam current was kept below 100 nA to prevent pile-up in the Ge(Li) detector. Protons were detected with two 1.5 mm Si surface-barrier detectors located at  $\theta_p = \pm 60^\circ$  with respect to the beam. Both detectors were covered with a  $100\text{ }\mu\text{m}$  mylar foil in order to stop the elastically scattered  $^3\text{He}$  particles. Gamma rays coincident with protons were detected with a Ge(Li) detector located at  $\theta_\gamma = 90^\circ$  and at 65 mm distance from the target.

For each coincidence event four digital words were generated, corresponding to the  $\gamma$ -ray energy (12 bits), the particle energy (10 bits), the time signal (7 bits), and a 2 bit word containing the routing information which indicated which of the two Si detectors received the event. A CDC-1700 computer system<sup>15)</sup> was used to collect the digitized information which was then stored, event by event, on magnetic tape. During data reduction, windows on the spectra were set by instructions to the analysing program. By appropriately restricting the dynamic range of the  $\gamma$ -ray signals for each particle group, time spectra were obtained with peaks having a FWHM of 4–5 ns. In most cases a 20 ns window was set on the time spectra.

The positions of the photopeaks were found from first-moment calculations. In some cases it was necessary to first subtract background due to Compton tails of higher-energy  $\gamma$ -rays. The energy dispersion and linearity of the  $\gamma$ -ray amplifier system and ADC were measured with  $^{22}\text{Na}$ ,  $^{60}\text{Co}$  and  $^{88}\text{Y}$  sources. With the measured

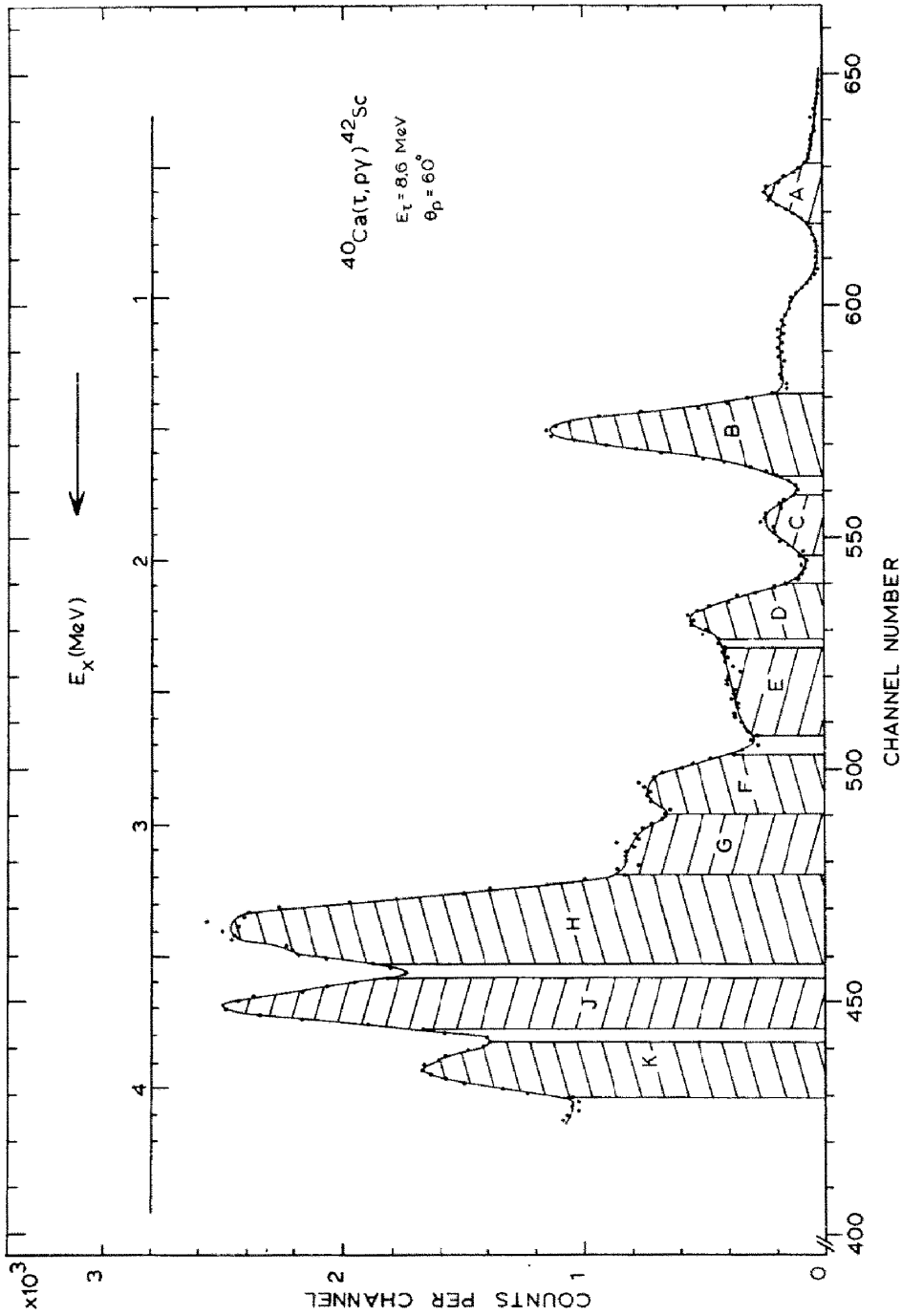


Fig. 1. Particle spectrum, detected at  $60^\circ$ , coincident with  $\gamma$ -rays between  $E_\gamma = 0.2$  and 4 MeV. The shaded areas indicate the particle windows used to generate coincidence  $\gamma$ -ray spectra. The measuring time for this spectrum was 4 d.

energy dispersion, the energies of the observed  $\gamma$ -rays were determined relative to the accurately known  $^{9,16})$   $611.1 \pm 0.4$  keV  $\gamma$ -ray which de-excites the first excited state of  $^{42}\text{Sc}$ .

Excitation curves for  $\theta_p = 60^\circ$  were measured for the reaction  $^{40}\text{Ca}(\tau, p)^{42}\text{Sc}$  from 7.0 to 10.0 MeV in steps of 200 keV. The overall resolution of  $\approx 150$  keV (FWHM) was mainly due to the target thickness and the mylar absorber. Though individual particle groups could not be resolved, these yield curves did indicate that in the energy range  $E_\tau = 8.2$ –8.8 MeV most of the states below 2.3 MeV were populated sufficiently strong for coincidence measurements. Subsequently, a set of coincidence runs ( $E_\tau = 8.2$ –8.8 MeV in 200 keV steps) were made with a  $12.7 \text{ cm} \times 12.7 \text{ cm}$  NaI(Tl) crystal ( $\theta_\gamma = 90^\circ$ ) and a 1.5 mm Si detector ( $\theta_p = 60^\circ$ ). Guided by the information obtained from these excitation curves, two lifetime measurements were performed: (i) a 2 d run at  $E_\tau = 8.4$  MeV with a  $36 \text{ cm}^3$  Ge(Li) detector and (ii) a 4 d run at  $E_\tau = 8.6$  MeV with a  $60 \text{ cm}^3$  detector.

The spectrum of protons coincident with  $\gamma$ -rays between  $E_\gamma = 0.2$  and 4 MeV recorded at  $E_\tau = 8.6$  MeV is shown in fig. 1. The shaded areas, labelled with the letters A through K, indicate the particle windows that were used to generate the coincidence  $\gamma$ -ray spectra. Only peak A contains a single proton group. For example, group B contains the triplet of levels near 1.5 MeV. The shoulder on the high-energy side of group B is due to accidental coincidences from the  $^{12}\text{C}(\tau, p_0)^{14}\text{N}$  reaction due to the carbon backing; group H is mainly from the reaction  $^{12}\text{C}(\tau, p_1)^{14}\text{N}$ .

### 3. Analysis

The Doppler shifts were determined from the differences between the peak centroids in the  $\gamma$ -ray spectra coincident with selected parts of the two proton spectra  $^{14})$ . The experimental Doppler-shift attenuation factor  $F(\tau_m)$  is defined as the ratio of the observed Doppler shift to the expected full shift. The full shift was calculated from reaction kinematics. The theoretical  $F(\tau_m)$  values  $^{17})$  are based on the nuclear stopping approximation of Blaugrund  $^{18})$  and the stopping-power theories of Lindhard, Scharff and Schiøtt  $^{19})$ . The quantity  $^{17,19})$   $\xi_e$  as extracted from experimental data on the slowing-down of ions in carbon  $^{20})$  was found to be  $\xi_e = 2.652 - 104 v/c$  for Sc ions. The statistical error in  $\tau_m$  was determined from the statistical uncertainty in  $F_{\text{exp}}(\tau_m)$ . The total error in the lifetime was then determined by quadratically adding to the statistical error the error due to an assumed uncertainty of  $\pm 20\%$  in the electronic stopping parameter of the target and backing and the error due to a  $10\%$  uncertainty in the target thickness. In most cases, the total error is dominated by the statistical part.

### 4. Experimental results

#### 4.1. EXCITATION ENERGIES

Gamma-ray spectra measured in coincidence with particle groups A through D are shown in figs. 2–5, respectively. These results obtained during the 4 d run at a

bombarding energy of 8.6 MeV are shown in order to illustrate the quality of the data. For example, the centroids of the photopeaks, such as those at 975 keV (fig. 3) and 1889 keV (fig. 4), can be measured with rather high accuracy, since there are no Compton tails from higher-energy  $\gamma$ -rays. This is true even though the area of the 1889 keV peak contains only about 40 counts. On the other hand, the centroid of the peak at 636 keV (fig. 5) cannot be determined accurately because of both the low yield and

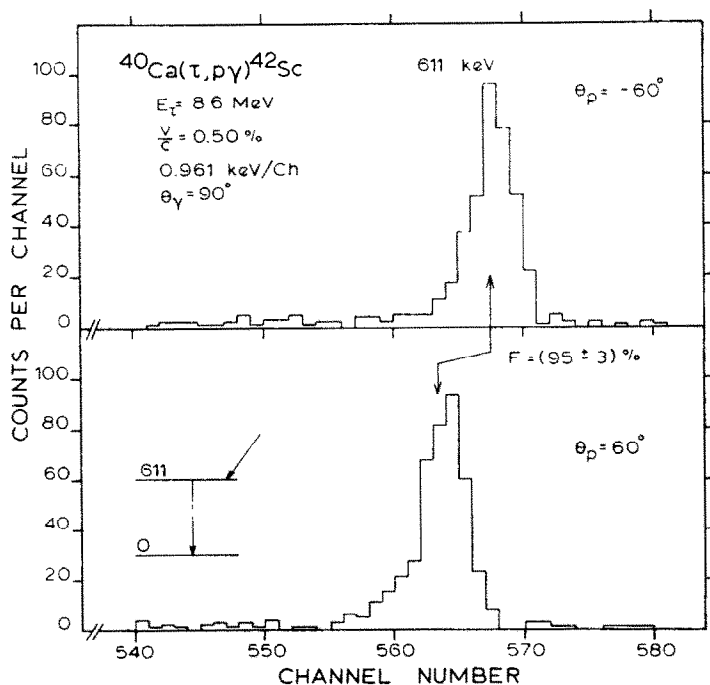


Fig. 2. The 611 keV  $\gamma$ -ray photopeaks, detected at  $90^\circ$ , coincident with particle group A (see fig. 1) at  $\theta_p = \pm 60^\circ$ . The peak centroids are indicated with joined arrows beside which is given the experimental  $F(\tau_m)$  in %.

the Compton tails from higher-energy  $\gamma$ -rays. The 683 keV  $\gamma$ -ray from the  $2270 \rightarrow 1587$  keV transition which has been observed previously by Nicholas *et al.*<sup>9)</sup> has very low yield at both 8.4 and 8.6 MeV.

The  $^{42}\text{Sc}$  excitation energies given in table 1 were calculated from the average of the  $\gamma$ -ray energies determined from the two Doppler-shifted peaks. The energy of the first excited state is taken from refs. <sup>9,16)</sup>. A  $20 \pm 1$  keV separation is taken from refs. <sup>5,8)</sup> for the 1491 and 1511 keV levels. In columns 2 and 3 of table 1 are also listed the excitation energies given by Sherr *et al.*<sup>8)</sup> and by Cline *et al.*<sup>7)</sup> which have an accuracy of about  $\pm 5$  and  $\pm 10$  keV, respectively. Uncertain levels are enclosed by parentheses. The energies obtained for eight levels by Nicholas *et al.*<sup>9)</sup> agree with those of the present experiment.

Part of the  $\gamma$ -ray spectrum coincident with particle group D (fig. 5) indicates a weak photopeak at  $710 \pm 2$  keV. A peak at this energy was also observed in the 8.4 MeV data. It was already noted <sup>8)</sup> that the excitation energy of 2297 keV given in ref. <sup>7)</sup> disagrees excessively with the excitation energy of 2270 keV [ref. <sup>9)</sup>]. This suggests that two levels exist <sup>8)</sup>, one at 2270 and another at 2297 keV. The 710 keV  $\gamma$ -ray could correspond to the  $2297 \rightarrow 1587$  keV, see table 1.

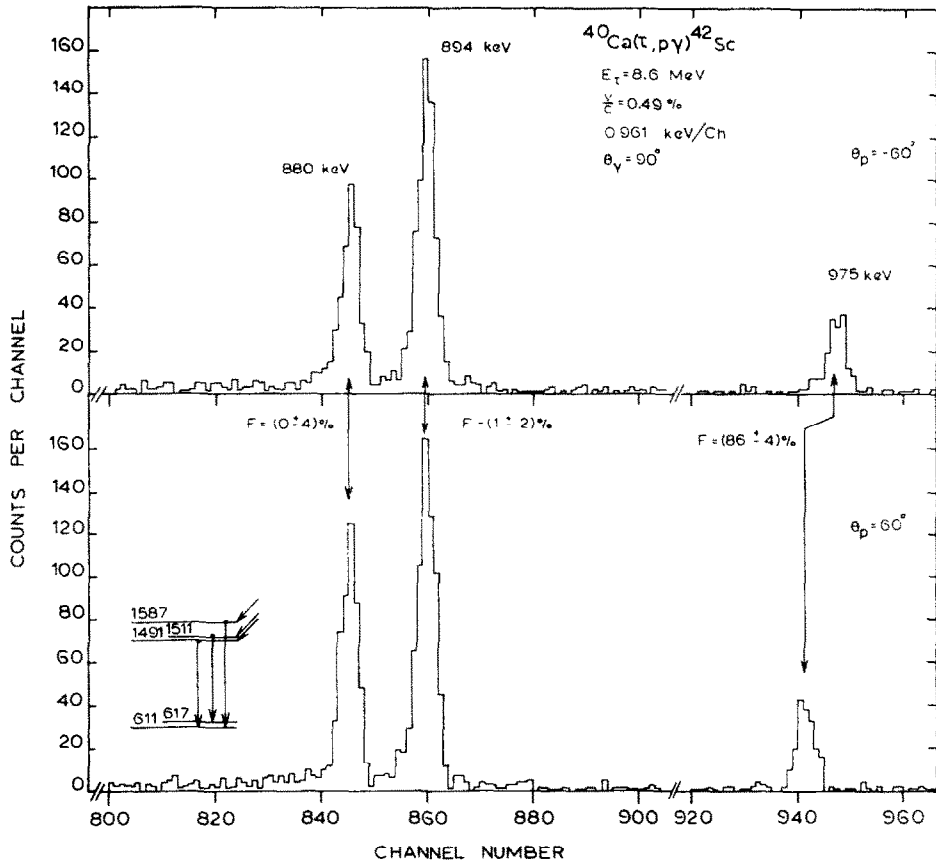


Fig. 3. The 880, 894 and 975 keV  $\gamma$ -ray photopeaks, detected at  $90^\circ$ , coincident with particle group B at  $\theta_p = \pm 60^\circ$ . The peak centroids are indicated with joined arrows beside which are given the experimental values of  $F(\tau_m)$  in %.

Since the level density is rather high above an excitation energy of 2.2 MeV, it is difficult to assign the observed  $\gamma$ -rays to particular transitions. Investigation of the  $\gamma$ -ray decay (see below) indicated that group J (fig. 1) is due, almost entirely, to protons leaving  $^{42}\text{Sc}$  in the excited state at 3.69 MeV. From kinematic calculations (including energy loss in the mylar foil) using the peaks corresponding to the excited states at 0.61, 1.49 + 1.51 and 3.69 MeV, the particle spectrum (see fig. 1) was calibrat-

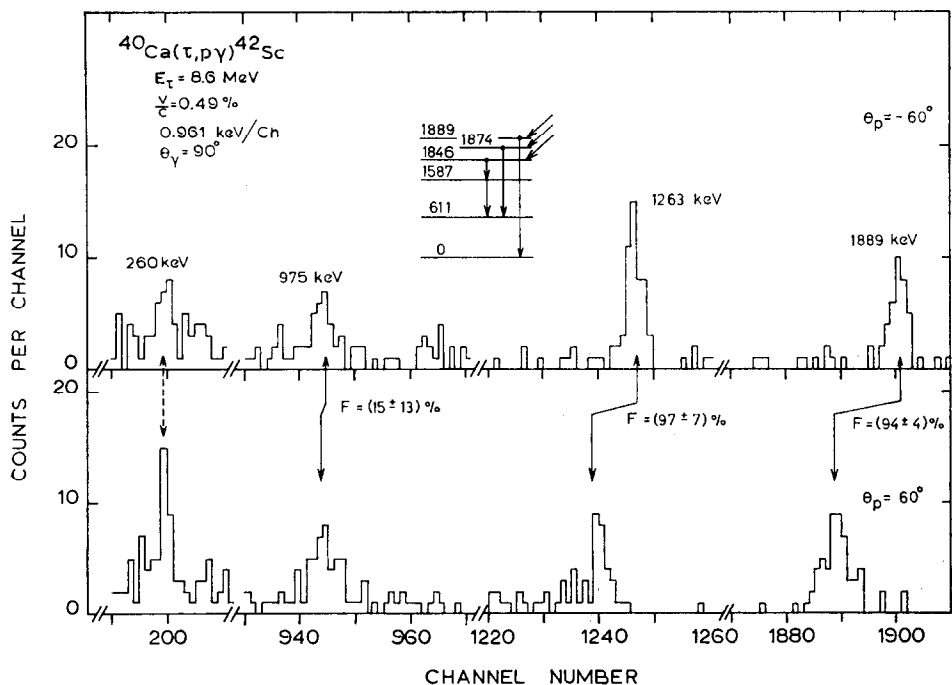


Fig. 4. The 260, 975, 1263 and 1889 keV  $\gamma$ -ray photopeaks, detected at  $90^\circ$ , coincident with particle group C at  $\theta_p = \pm 60^\circ$ . The peak centroids of the peaks are marked with joined arrows beside which are given the experimental values of  $F(\tau_m)$  in %. Dashed joined errors indicate that a value of  $F(\tau_m)$  was not obtained in this experiment.

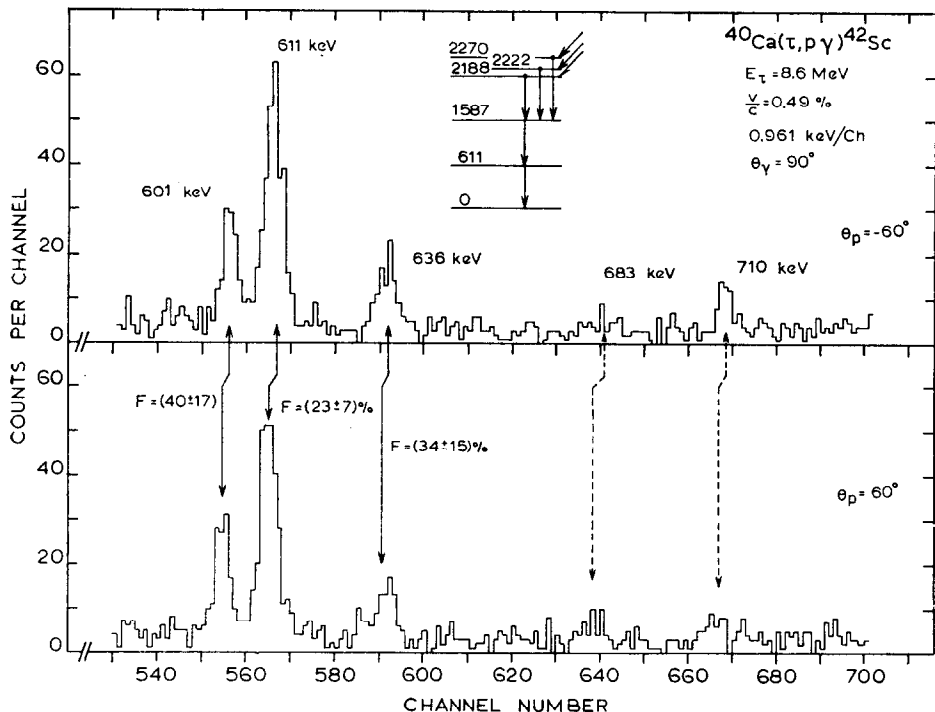


Fig. 5. The 601, 611, 636, 683 and 710 keV  $\gamma$ -ray photopeaks, detected at  $90^\circ$ , coincident with particle group D at  $\theta_p = \pm 60^\circ$ . The centroids of the peaks are marked with joined arrows beside which are given the experimental values of  $F(\tau_m)$  in %. Dashed joined arrows indicate that a value of  $F(\tau_m)$  was not obtained in this experiment. Only some of the known  $\gamma$ -ray transitions are shown in the inserted energy level diagram.

TABLE I  
Excitation energies, observed values of  $F(\tau_m)$  and deduced mean lives

$E_x$ (keV)			$E_\gamma$ <sup>a)</sup> (keV)	$F(\tau_m)$ (%)		$\tau_m$ (fs)	
This work <sup>b)</sup>	( $\tau$ , t) ref. <sup>8)</sup>	( $\tau$ , p) ref. <sup>7)</sup>		8.4 MeV	8.6 MeV	This work <sup>b)</sup>	ref. <sup>13)</sup>
611.1 $\pm$ 0.4 <sup>c)</sup>	615	618	611.1 $\pm$ 0.4 <sup>c)</sup>	92 $\pm$ 5	95 $\pm$ 3	41 $\pm$ 17	140 $\pm$ 30
617.3 $\pm$ 1.3	625						
1491.1 $\pm$ 0.6	1498		880.0 $\pm$ 0.4	3 $\pm$ 3	0 $\pm$ 4	> 4000 <sup>c)</sup>	> 5000 <sup>b)</sup>
1511.1 $\pm$ 1.2	1518	1505 <sup>d)</sup>	893.8 $\pm$ 0.4	4 $\pm$ 4	1 $\pm$ 2	> 6000 <sup>c)</sup>	> 5000 <sup>b)</sup>
1586.5 $\pm$ 0.6	1593	1589	{ 1586.1 $\pm$ 1.1 975.4 $\pm$ 0.4	84 $\pm$ 7	{ 80 $\pm$ 11 86 $\pm$ 4	100 $\pm$ 30	86 $\pm$ 40
1846 $\pm$ 2	1844	1847	260 $\pm$ 2	10 $\pm$ 11 <sup>f)</sup>	15 $\pm$ 13 <sup>f)</sup>	> 1000 <sup>g)</sup>	
1873.6 $\pm$ 0.8			1262.5 $\pm$ 0.7	120 $\pm$ 30	97 $\pm$ 7	< 100	
1889.0 $\pm$ 0.8	1888 <sup>d)</sup>	1895 <sup>d)</sup>	1889.0 $\pm$ 0.8	96 $\pm$ 4	99 $\pm$ 4	< 60	60 $\pm$ 35
2187.6 $\pm$ 0.7	2185	2186	601.3 $\pm$ 0.4	35 $\pm$ 17	40 $\pm$ 17	780 $\pm$ 350	
2222.4 $\pm$ 0.8 <sup>i)</sup>	2222	2220	2222.6 $\pm$ 1.3		82 $\pm$ 6	125 $\pm$ 50	
			635.9 $\pm$ 0.5	39 $\pm$ 27	34 $\pm$ 15	900 $\pm$ 500	
2270 $\pm$ 2	2262		{ 1661 $\pm$ 3 683 $\pm$ 2				
2297 $\pm$ 2 *		2297	710 $\pm$ 2				
2455 $\pm$ 2 *		2461	2455 $\pm$ 2		65 $\pm$ 14	260 $\pm$ 160	
2488.2 $\pm$ 1.0	2482	2501	1877.1 $\pm$ 0.9	78 $\pm$ 11	100 $\pm$ 5	< 70	
2535 $\pm$ 2 *		2544	2535 $\pm$ 2		39 $\pm$ 9	950 $\pm$ 400	
2586.8 $\pm$ 1.7*		2589	1095.7 $\pm$ 1.6				
2650.3 $\pm$ 1.3*	2650	2655	1064.0 $\pm$ 1.1		58 $\pm$ 25	480 $\pm$ 350	
2816.5 $\pm$ 1.5	2812	2807	1305.4 $\pm$ 0.7	97 $\pm$ 11	103 $\pm$ 8	< 100	
2832.9 $\pm$ 1.1*			1246.6 $\pm$ 0.9		59 $\pm$ 13	300 $\pm$ 160	
2847.5 $\pm$ 1.3*	(2844) <sup>d)</sup>	2846	1261.2 $\pm$ 1.1		65 $\pm$ 17	290 $\pm$ 180	
2910.1 $\pm$ 1.4*	2907 <sup>d)</sup>	2919	1419.0 $\pm$ 1.2		0 $\pm$ 12	> 1200	
3089.7 $\pm$ 1.6	(3080)	3090	2472.4 $\pm$ 1.0	65 $\pm$ 6	57 $\pm$ 4	300 $\pm$ 60	
3392.7 $\pm$ 1.1	3380	3394	{ 904.5 $\pm$ 0.5 575.9 $\pm$ 1.2	101 $\pm$ 11	87 $\pm$ 9	90 $\pm$ 70	
3687.8 $\pm$ 0.8	(3670)	3695	{ 3689 $\pm$ 2 2101.2 $\pm$ 1.0 1813.5 $\pm$ 1.1		{ 93 $\pm$ 8 98 $\pm$ 2 99 $\pm$ 5	< 40	
3933.5 $\pm$ 1.4	(3938)	3934	2347.1 $\pm$ 1.3		97 $\pm$ 4	< 75	

<sup>a)</sup> In the  $E_x = 8.6$  MeV experiment also an  $E_\gamma = 1324.5 \pm 1.0$  keV  $\gamma$ -ray was observed coincident with protons to  $E_x \approx 2.8$  MeV.

<sup>b)</sup> Excitation energies marked with an asterisk indicate uncertain  $\gamma$ -ray assignments.

<sup>c)</sup> Average for  $E_\gamma$  from refs. <sup>9, 16)</sup>.

<sup>d)</sup> Doublet.

<sup>e)</sup> Upper limit 3 ns.

<sup>f)</sup> The  $F(\tau_m)$  was obtained from the 975 keV cascade  $\gamma$ -ray following the 260 keV transition.

<sup>g)</sup> Upper limit 5 ns [ref. <sup>24)</sup>].

<sup>h)</sup> Average values. For errors see subsect. 4.2.

<sup>i)</sup> Possibly a doublet, see subsect. 4.2.

<sup>j)</sup> Ref. <sup>27)</sup>.



ed in terms of the excitation energy in  $^{42}\text{Sc}$ . With the aid of this calibration and the previously reported excitation energies (and cross sections), a number of the observed  $\gamma$ -rays were assigned to specific transitions. Unfortunately, for a number of the low-yield  $\gamma$ -rays observed in the 8.6 MeV data, several possibilities exist.

In an attempt to determine more closely the excitation energy of the levels associated with the measured  $\gamma$ -rays, the data for particle groups E and F were re-analysed

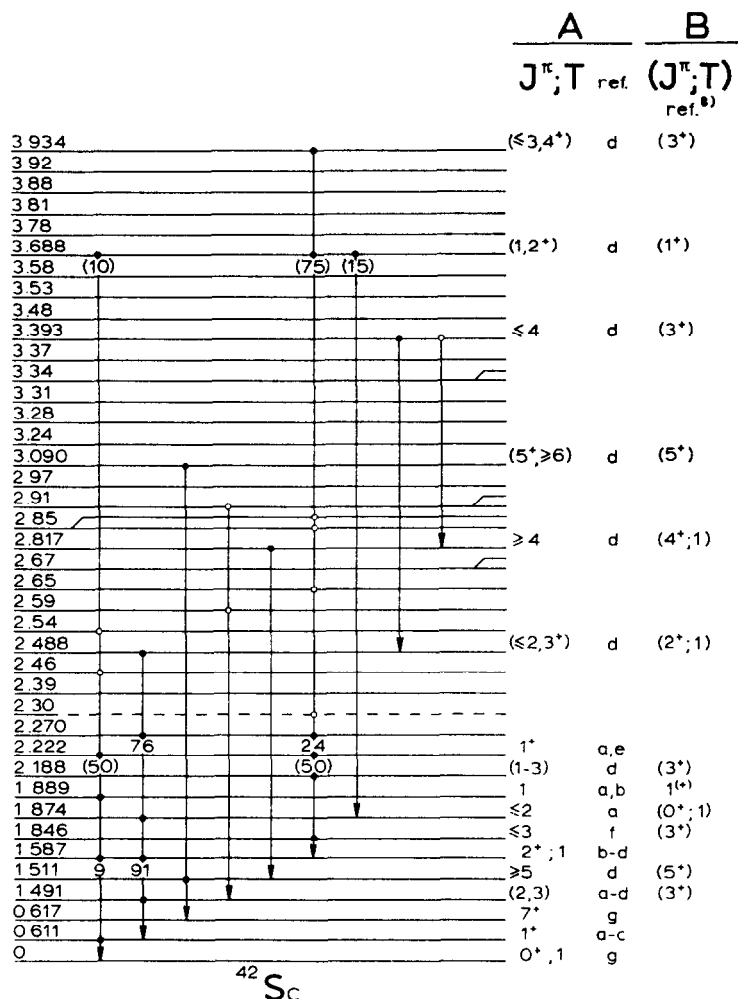


Fig. 6. Level scheme of  $^{42}\text{Sc}$  with the  $\gamma$ -ray transitions studied in the present work. Uncertain transitions are indicated by open circles. The excitation energies are from this work for the levels with assigned  $\gamma$ -ray transitions. For all other levels the energies are from refs. <sup>7, 8</sup>). Doublets (or multiplets) are indicated by double lines. Spins, parities and isospins are only given for levels from or to which  $\gamma$ -ray decay is observed. In column A definite  $J^\pi$  and  $T$  values or limits on  $J^\pi$  are given. Refs. <sup>a-c</sup>) correspond to refs. <sup>9, 12, 13</sup>), respectively, refs. <sup>e-g</sup>) to refs. <sup>16, 24, 11</sup>), respectively, whereas <sup>d</sup>) indicates this work. Further, uncertain  $J^\pi$  and  $T$  assignments <sup>8</sup>) are given in column B.

with narrower windows on the particle spectra. Coincidence  $\gamma$ -ray spectra were obtained with one 10-channel particle window (180 keV) which was stepped through the particle groups in 5-channel steps (90 keV). From the yield of a  $\gamma$ -ray as a function of window position, it was possible to determine the energy of the associated particle group to approximately 100 keV. Also, it was possible to determine relative excitation energies, to within about 50 keV.

In all but one case (the 1325 keV  $\gamma$ -ray), the excitation energy was exact enough to assign the measured  $\gamma$ -rays to *known* levels. Obviously, these assignments cannot all be considered unique, as many of the known levels in  $^{42}\text{Sc}$  are still uncertain by  $\pm 10$  keV [refs. <sup>7,8</sup>], and the possibility of unreported levels cannot be ruled out. Uncertain assignments are indicated in table 1 by marking the excitation energies with an asterisk. Since in this experiment the determined values of  $\tau_m$  are rather insensitive to the excitation energy (i.e. recoil velocity), the mean lives given in table 1 will not be affected appreciably if the assignment is changed at a later time.

The level diagram shown in fig. 6 summarizes the information about  $^{42}\text{Sc}$ . The excitation energies are taken from this work for those levels with assigned  $\gamma$ -ray transitions. For all other levels (including the levels with uncertain  $\gamma$ -ray assignments), the excitation energies are from refs. <sup>7,8</sup>). For spins, parities and isospins see caption of fig. 6; the branching ratios are from refs. <sup>9,12</sup>), the ones in parentheses are relative intensities from this work, see sect. 1.

The  $\gamma$ -ray assignments for the levels below  $E_x = 2.27$  MeV are straightforward and the results of this experiment agree with those of refs. <sup>9,12</sup>).

The 1877, 905, 1814, 2101, 3689 and 2347 keV  $\gamma$ -rays are indicated as assigned transitions from states at 2.49, 3.39, 3.69 and 3.93 MeV. In these cases, cascade  $\gamma$ -rays were observed with the appropriate intensities and the determined excitation energies could be associated with levels known to have relatively large ( $\tau$ ,  $p$ ) cross sections <sup>6,7</sup>). The measured excitation energy associated with the 2472 keV  $\gamma$ -ray permitted an assignment as a transition either to the 0.62 or the 0.61 MeV level. Since the 611 keV  $\gamma$ -ray intensity is too low to be the secondary, the 2472 keV  $\gamma$ -ray de-excites the level at 3.09 MeV to the isomeric second excited state at 0.62 MeV.

In the case of the 1305 keV transition which was observed in both the 8.4 and 8.6 MeV data, the associated particle energy indicates that the only possible transitions are  $2817 \rightarrow 1511$  or  $2797 \rightarrow 1491$  keV. An excitation energy of 2797 keV disagrees with the systematic trend of the deviations between the excitation energies determined in this work and those of Sherr *et al.* <sup>8</sup>). On the other hand, an excitation energy of 2817 keV agrees quite well, such that the 1305 keV  $\gamma$ -ray is assigned as a  $2817 \rightarrow 1511$  keV transition. The observed intensity of the 894 keV secondary  $\gamma$ -ray also supports this assignment.

The 1325 keV  $\gamma$ -ray [see table 1, footnote <sup>a</sup>)] could be the  $2817 \rightarrow 1491$  keV transition. However, since this  $\gamma$ -ray is not seen in the 8.4 MeV data, it cannot, therefore, decay from the same level ( $E_x = 2.82$  MeV) as the 1305 keV  $\gamma$ -ray which was observed at both  $E_\tau = 8.4$  and 8.6 MeV.

The possibility exists that some of the  $\gamma$ -rays discussed above are from target contaminants; this is a problem primarily for the levels above 2.27 MeV. The most likely  $\gamma$ -rays from the  $(\tau, p)$  and  $(\tau, d)$  reactions on the isotopes of C, N, O, F, Na, Mg, Cl and Ca were calculated from the known excitation energies and branching ratios [refs. <sup>11, 21-23</sup>]. For all but one of the cases, the possible contaminant  $\gamma$ -ray could be eliminated because either: (i) the other member(s) of a cascade or branch was not observed, (ii) kinematic calculations indicated that the  $\gamma$ -ray could not be in the coincidence spectrum, or (iii) the observed mean life was not correct.

The remaining case is that of  $\gamma$ -rays from  $^{46}\text{Sc}$  produced by the  $(\tau, p)$  reaction on  $^{44}\text{Ca}$  (2 % natural abundance). Two low-yield  $\gamma$ -rays with energies of 711 and 1058 keV have been observed via thermal-neutron capture in scandium but are not assigned to specific  $^{46}\text{Sc}$  levels. Since no other  $\gamma$ -rays have been observed that can be associated with any of the numerous levels of  $^{46}\text{Sc}$ , contamination from the  $^{44}\text{Ca}(\tau, p)$  reaction seems unlikely.

#### 4.2. MEAN LIVES

Table 1 also lists the experimental  $F(\tau_m)$  values obtained at 8.4 and 8.6 MeV. The errors shown for  $F(\tau_m)$  are only statistical, but the mean lives include the effects of the uncertainty of the electronic stopping and target thickness (see sect. 3). Limits were determined from the  $F(\tau_m)$  curves at twice the assigned errors. Also shown in table 1 are the results of another recent lifetime measurement <sup>13</sup>). But for the first excited state, the agreement is good. The upper limits for the 1.49 and 1.51 MeV levels were obtained from the time spectra. While the yield to the 1.85 MeV level was too low in this experiment for an upper limit to be obtained from the time spectrum, a recent measurement by Gould *et al.* <sup>24</sup>) with the  $^{39}\text{K}(\alpha, n\gamma)^{42}\text{Sc}$  reaction, determined a value of 5 ns for this limit.

It should be noted that the level at 2.22 MeV has two lifetimes listed in table 1. The  $F(\tau_m)$  determined from the 8.6 MeV data for the 2223 keV  $\gamma$ -ray is  $(82 \pm 6)\%$ , while the values for the 636 keV  $\gamma$ -ray are  $(39 \pm 27)\%$  and  $(34 \pm 15)\%$  at 8.4 and 8.6 MeV, respectively. The difference between the  $F(\tau_m)$  values obtained from the two  $\gamma$ -rays is, for the 8.6 MeV data, over two times the assigned errors. This suggests the possibility of two levels near 2.22 MeV with either the two  $\gamma$ -rays representing the decay from different states or with a third  $\gamma$ -ray with an energy near 636 keV. In this case, the two levels would have to occur within about 5 keV of each other. Clearly more experimental work needs to be carried out for the levels near 2.2 MeV. Since the 2223 keV  $\gamma$ -ray is in a very clean region with basically no background (or Compton tails), the  $F(\tau_m)$  of  $(82 \pm 6)\%$  will be assumed for the 2.22 MeV level in the following.

On the basis of the mean lifetimes, branching ratios and the distribution of transition strengths <sup>25</sup>), limits can be placed on possible spins (see fig. 6).

### 5. Comparison of theoretical calculations and experimental results

Because the calculations by Flowers and Skouras <sup>1)</sup> (FS) include more configurations than earlier shell-model calculations <sup>6, 26)</sup>, and since Schaeffer <sup>10)</sup> has recently used these wave functions in a microscopic analysis of the  $^{42}\text{Sc}(\tau, t)^{42}\text{Sc}$  reaction,

TABLE 2

Comparison of experimental branching ratios and mean lives of even-parity levels in  $^{42}\text{Sc}$  with the theoretical calculations of Flowers and Skouras (FS) [ref. <sup>1)</sup>]

$E_{x1}$ (MeV)	$E_{x2}$ (MeV)	$(J\pi m)^a$		Branching ratio (%)		$\tau_m$	
		initial	final	(FS)	exp. <sup>b)</sup>	(FS)	this work
0.61	0	(101)	(011)	100	100	47 fs	$41 \pm 17$ fs
1.49	0.61	(301)	(101)	100	100	440 ps	$4 \text{ ps} < \tau < 3 \text{ ns}$
1.49	0.61	(302)	(101)	100	100	20 ps	$4 \text{ ps} < \tau < 3 \text{ ns}$
1.51	0.62	(501)	(701)	100	100	21 ps	$6 \text{ ps} < \tau < 3 \text{ ns}$
1.59	0.61	(211)	(101)	90	91	100 fs	$100 \pm 30$ fs
	0		(011)	10	9		
1.85	1.59	(302)	(211)	80	(100)	700 fs	$1 \text{ ps} < \tau < 5 \text{ ns}$
	0.61		(101)	20			
1.85	1.59	(301)	(211)	38	(100)	49 ps	$1 \text{ ps} < \tau < 5 \text{ ns}$
	1.49		(302)	2			
	0.61		(101)	60			
1.87	0.61	(012)	(101)	100	100	40 fs	$< 100$ fs
1.89	1.59	(102)	(211)	1		24 fs	$< 60$ fs
	0		(011)	99	100		
2.19	1.59	(303)	(211)	100	100	1500 fs	$780 \pm 350$ fs
2.22	1.87	(103)	(012)	18		700 fs	$125 \pm 50$ fs <sup>c)</sup>
	1.59		(211)	56	(50)		
	0.61		(101)	25			
	0		(011)	$< 2$	(50)		
2.49	1.49	(212)	(302)	22		7 fs	$< 70$ fs
	0.61		(101)	77	(100)		
2.82	2.19	(411)	(303)	1		4 fs	$< 100$ fs
	1.51		(501)	82	(100)		
	1.49		(302)	17			
3.09	2.19	(502)	(303)	4		1900 fs	$300 \pm 55$ fs
	1.85		(301)	86			
	1.51		(501)	2			
	1.49		(302)	8			
	0.62		(701)		(100)		

<sup>a)</sup> The notation  $(J\pi m)$  denotes the  $m$ th state with spin  $J$  and isospin  $T$ .

<sup>b)</sup> Numbers in parentheses are relative intensities from this experiment. The unbracketed branching ratios are from refs. <sup>9, 12)</sup>.

<sup>c)</sup> See subsect. 4.2.

the results of this experiment will be compared with the electromagnetic decay rates predicted by the Flowers and Skouras model. While very little experimental information was available in 1969, Flowers and Skouras <sup>1)</sup> conveniently included the calculated M1 and E2 reduced matrix elements in their publication. In order to facilitate a comparison with theory the  $(J^\pi, T)$  values <sup>8)</sup> (which are still uncertain) as given

in column B of fig. 6 are used. Table 2 compares the experimental branching ratios and lifetimes with those predicted from the M1 and E2 matrix elements. The numbers listed in the column 6 and enclosed in parentheses are the intensity ratios observed in this experiment. The (FS) notation is used to label the states in table 2; ( $JTm$ ) denotes the  $m$ th state with a specific  $J, T$  value. Only transitions with a branching ratio greater than 1 % are tabulated. In some cases more than one initial state is considered. For example, the 1491 keV level is compared with both the (301) and (302) states.

### 5.1. THE $T = 1$ LEVELS

5.1.1. *The 1.87 MeV  $0^+$  state.* From ref. <sup>9)</sup> it is known that at  $E_x = 1.88$  MeV there is a close doublet. This and the  $\gamma$ -ray decay of the components is confirmed in the present work (see fig. 6). From angular correlation measurements <sup>9, 12)</sup> it follows that the 1.87 and 1.89 MeV levels have  $J \leq 2$  and 1, respectively.

From the mean-life limit of the  $E_x = 1.87$  MeV state ( $\tau_m < 100$  fs) it follows that the  $1.87 \rightarrow 0.61$  MeV transition would have a strength of at least  $4.0 \times 10^{-3}$  W.u. if it were of E1 character. The logarithmic average of the strength of the twenty known E1 ( $\Delta T = 0$ ) transitions in  $A = 2Z$  nuclei in the region  $Z = 3-21$  is  $4.7 \times 10^{-5}$  W.u., the strongest transition has  $2.2 \times 10^{-3}$  W.u. [ref. <sup>23)</sup>]. Although from the above arguments odd parity for the 1.87 MeV state cannot be excluded definitely, it seems reasonable to assume even parity. In that case the  $1.87 \rightarrow 0.61$  MeV transition has an M1 strength of at least 0.12 W.u. (the E2 strength is assumed less than 60 W.u.). For the 31 known delayed ( $\Delta T = 0$ ) M1 transitions in  $A = 2Z$  nuclei in the  $Z = 3-21$  region the logarithmic average of the strength is  $7.3 \times 10^{-4}$  and the strongest transition has  $1.2 \times 10^{-2}$  W.u. [ref. <sup>23)</sup>]. From this it may be concluded that the  $1.87 \rightarrow 0.61$  MeV transition is of  $\Delta T = 1$  character. From a comparison with the  $^{42}\text{Ca}$  level scheme this would lead to a  $J^\pi = 0^+, T = 1$  assignment for the  $E_x = 1.87$  MeV state.

The lifetime limit is consistent with the theoretical value of 40 fs based on a (012)  $\rightarrow$  (101) transition.

5.1.2. *The  $2^+$  and  $4^+$  states.* From angular-correlation measurements <sup>12)</sup> combined with mean-life measurements [see also ref. <sup>13)</sup>] it follows that the  $E_x = 1.59$  MeV level has  $J^\pi = 2^+$ . From the mixing ratio <sup>13)</sup>, the branching ratio <sup>12)</sup> and the mean life the M1 strength for the  $1.59 \rightarrow 0.61$  MeV transition is found as  $0.31 \pm 0.08$  W.u. From this it is concluded (see subsect. 5.1.1) that this transition is of  $T$ -favored M1 character, which yields  $T = 1$  for the 1.59 MeV level.

The 2.49 MeV state has  $\tau_m < 70$  fs. This limit does not show that the  $2.49 \rightarrow 0.61$  MeV transition is of  $T$ -favored M1 character; it can also be E1 or E2. For comparison with theory  $J^\pi = 2^+, T = 1$  is assumed <sup>8)</sup> for this state.

It is seen in table 2 that the observed branching ratio and mean life of the 1.59 MeV state agree well with theory. Also, the predicted mean life and branching ratio of the (212) state are consistent with experiment.

Theory predicts the (411) state ( $\tau_m = 4$  fs) to decay mainly to the (501) state, see

table 2. This is in good agreement with the experimental results for the 2.82 MeV level. Correspondence with the (401) state is ruled out, because of the predicted mean life of 35 ps.

## 5.2. THE $T = 0$ LEVELS

5.2.1. *The  $1^+$  states.* The levels at  $E_x = 0.61$ , 2.22 and 1.89 MeV are known to have  $J^\pi = 1^+$ ,  $1^+$  and 1, respectively, see fig. 6. For comparison with theory it is assumed that the latter has even parity<sup>8)</sup>.

The agreement with theory is good for the 0.61 and 1.89 MeV levels when the association is made with the (101) and (102) states, respectively. The predictions for the (103) state are at variance with the measured properties of the 2.22 MeV state (see also subsect. 4.2).

No comparison can be made for the 3.69 MeV state, since the transition probabilities for higher  $1^+$  states are not given in ref. <sup>1)</sup>. This state mainly decays to the 1.59 MeV,  $T = 1$  state and weakly to the  $T = 1$  ground state and the 1.87 MeV,  $T = 1$  state. This, together with the lifetime limit ( $\tau_m < 40$  fs), suggests  $T = 0$  for the 3.69 MeV state. It should also be noted that this level has the highest yield of any observed in this experiment. This fact along with the properties of the  $\gamma$ -ray decay indicate that the wave function of this state must contain strong admixtures of (fp) configurations (see ref. <sup>1)</sup> for the wave functions of the ground state and the 1.59 and 1.87 MeV states).

5.2.2. *The  $3^+$  and  $5^+$  states.* None of these states have been rigorously located (see fig. 6), such that also in this discussion the  $J^\pi$  values from ref. <sup>8)</sup> will be used.

It has been suggested<sup>10)</sup> that the wave functions of the lowest two  $3^+$  (FS) states should be interchanged. Therefore, the 1.49 and 1.85 MeV states are compared with both the (301) and (302) states. Unfortunately, no preference for identification can be made on the basis of the present mean-life limits. A lifetime measurement of the 1.49 MeV level with the recoil-distance method should be able to resolve this difficulty.

The comparison of the state at 2.19 MeV with the (303) state shows reasonable agreement.

The lifetime limits on the 3.39 and 3.93 MeV states  $J^\pi = (3^+)$  suggest  $\Delta T = 1$  M1 character for the de-exciting transitions. Here, calculations are not available.

The (501) states could correspond to the 1.51 MeV state. Again, a recoil-distance measurement would be useful.

It has been suggested<sup>6,10)</sup> that the 3.09 MeV state, which has  $\tau_m = 300 \pm 60$  fs, has the  $f_{7/2}p_{3/2}$  configuration as the main component. The only (FS) state available for comparison is (502), which contains very little shell-model strength. From table 2 it can be seen that indeed the (502) state cannot be associated with the 3.09 MeV level.

## 5.3. CONCLUSION

It has been shown that the observed electromagnetic transition rates agree rather well with the calculations of Flowers and Skouras<sup>1)</sup>, and in general support the cor-

respondences proposed by Schaeffer <sup>10</sup>). Since the fitted parameters, including the effective charge, were taken to have the same values as those used in their  $^{42}\text{Ca}$  calculation, Flowers and Skouras <sup>1</sup>) have already pointed out that small changes in these parameters may give still better agreement.

The authors wish to thank Prof. P. M. Endt for stimulating discussions and useful suggestions and Prof. A. M. Hoogenboom for his continuous interest in this work.

This work was performed as part of the research programme of the "Stichting voor Fundamenteel Onderzoek der Materie" (FOM) with financial support from the "Nederlandse Organisatie voor Zuiver Wetenschappelijk Onderzoek (ZWO)".

### References

- 1) B. H. Flowers and L. D. Skouras, Nucl. Phys. **A136** (1969) 353
- 2) R. W. Zurmühle, C. M. Fou and L. W. Swenson, Nucl. Phys. **80** (1966) 259
- 3) J. Kim, Phys. Soc. Jap. **21** (1966) 2445
- 4) E. Rivet, R. H. Pehl, J. Cerny and B. J. Harvey, Phys. Rev. **141** (1966) 1021
- 5) J. J. Schwartz *et al.*, Phys. Rev. Lett. **19** (1967) 1482
- 6) F. Pühlhofer, Nucl. Phys. **A116** (1968) 516
- 7) D. Cline, H. E. Gove and B. Cujec, Bull. Am. Phys. Soc. **10** (1965) 25, and as quoted by Sherr *et al.* in ref. <sup>8</sup>)
- 8) R. Sherr, T. S. Bhatia, D. Cline and J. J. Schwartz, Phys. Rev., to be published
- 9) F. M. Nicholas *et al.*, Nucl. Phys. **A124** (1969) 97
- 10) R. Schaeffer, Nucl. Phys. **A164** (1971) 145
- 11) P. M. Endt and C. van der Leun, Nucl. Phys. **A105** (1967) 1
- 12) D. P. Balamuth, G. P. Anastassiou and R. W. Zurmühle, Phys. Rev. **C2** (1970) 215
- 13) H. Grawe, R. Hartmann and K. Kädler, Conf. on the structure of  $f_{7/2}$  nuclei, Padova, 1971
- 14) G. A. P. Engelbertink and G. van Middelkoop, Nucl. Phys. **A138** (1969) 588
- 15) P. B. J. van Elswijk, R. Engmann, A. M. Hoogenboom and P. de Wit, Nucl. Instr. **96** (1971) 35
- 16) A. Gallmann, E. Aslanides, F. Jundt and E. Jacobs, Phys. Rev. **186** (1969) 1160
- 17) G. van Middelkoop and C. J. Th. Gunsing, Nucl. Phys. **A147** (1970) 225
- 18) A. E. Blaugrund, Nucl. Phys. **88** (1966) 501
- 19) J. Lindard, M. Scharff and H. E. Schiøtt, Mat. Fys. Medd. Dan. Vid. Selsk. **33** (1963) no. 14
- 20) D. Hvelplund and B. Fastrup, Phys. Rev. **165** (1968) 408
- 21) F. Ajzenberg-Selove and T. Lauritsen, Nucl. Phys. **11** (1959) 1
- 22) F. Ajzenberg-Selove, Nucl. Phys. **A152** (1970) 1
- 23) From recent refs. compiled by P. M. Endt and C. van der Leun
- 24) C. R. Gould, Duke University, USA, private communication
- 25) S. J. Skorka, J. Hertel and T. W. Retz-Schmidt, Nucl. Data **A2** (1966) 347
- 26) T. T. S. Kuo and G. E. Brown, Nucl. Phys. **A114** (1968) 241
- 27) C. R. Gould *et al.*, Bull. Am. Phys. Soc. **16** (1971) 555